

Supporting Information

Solvatomorphism of Reichardt's Dye

Sarah J. Pike, Andrew D. Bond, Christopher A. Hunter*

Department of Chemistry, University of Cambridge, Cambridge, CB2 1EW, U.K.

Email: herchelsmith.orgchem@ch.cam.ac.uk

Contents	<i>S2</i>
General Experimental Section	<i>S3</i>
Recrystallisation Conditions	<i>S3</i>
Crystallographic data	<i>S4</i>
Summary of structure types for Reichardt's dye	<i>S6</i>
Intermolecular interactions in the hexagonal channel structure	<i>S7</i>
Intermolecular interactions in the chlorobenzene/4-methylanisole structures	<i>S8</i>
Polar aprotic O-containing solvents: acetone and dioxane	<i>S10</i>
Protic solvents: ethylene glycol, EtOH, ⁱPrOH, H₂O(MeOH), CHCl₃/H₂O	<i>S12</i>
Tunnel Calculations using CAVER 3.0	<i>S19</i>
References	<i>S30</i>

General Experimental Section

Reichardt's dye, Et₂O and chlorobenzene were purchased from Sigma-Aldrich. Acetonitrile, 1,4-dioxane, acetone and chloroform were purchased from Acros as 99+% for spectroscopic grade. Ethylene glycol, dichloromethane, hexane and methanol were purchased from Fisher. Ethanol was purchased from VWR Chemicals. All reagents and chemicals were used as received.

The following abbreviation is used: Et = ethyl.

Recrystallization Conditions

Two crystallization methods were employed for the growth of single crystals: (i) slow evaporation of a solution of Reichardt's dye; (ii) vapour diffusion of *n*-hexane or diethyl ether into a solution of Reichardt's dye.

Single-crystal X-ray diffraction data were collected on a Bruker D8-QUEST PHOTON-100 diffractometer equipped with an Incoatec I μ S Cu microsource. Data integration and reduction were carried out using SAINT within the APEX3 software suite. Multi-scan empirical absorption corrections were applied using SADABS. Structures were solved using SHELXT and refined using full-matrix least squares on F² using SHELXL-2018/1.

Crystallographic data: structures handled by conventional refinement

	Acetone solvate (1:1)	Dioxane solvate (1:2)	Chlorobenzene (1:1)	Ethylene glycol solvate (2:3)	CHCl ₃ /H ₂ O solvate (1:0.625:1.25)	H ₂ O(MeOH) solvate ^a
CCDC number	1827182	1827192	1827190	1827184	1827187	1827189
Empirical formula	C ₄₄ H ₃₅ NO ₂	C ₄₉ H ₄₅ NO ₅	C ₄₇ H ₃₄ ClNO	C ₄₄ H ₃₈ NO ₄	C _{41.62} H _{32.12} Cl _{1.88} NO _{2.25}	C ₄₁ H ₃₃ NO ₃
Moiety formula	C ₄₁ H ₂₉ NO, C ₃ H ₆ O	C ₄₁ H ₂₉ NO, 2(C ₄ H ₈ O ₂)	C ₄₁ H ₂₉ NO, C ₆ H ₅ Cl	C ₄₁ H ₂₉ NO, 1.5(C ₂ H ₆ O ₂)	C ₄₁ H ₂₉ NO, 1.25(H ₂ O), 0.625(CHCl ₃)	C ₄₁ H ₂₉ NO, 2(H ₂ O)
Formula weight	609.73	727.86	664.20	644.75	648.78	587.68
Temperature / K	180(2)	180(2)	180(2)	180(2)	180(2)	180(2)
Crystal system	monoclinic	monoclinic	monoclinic	monoclinic	triclinic	triclinic
Space group	<i>P</i> 2 ₁ / <i>n</i>	<i>C</i> 2/ <i>c</i>	<i>P</i> 2 ₁ / <i>n</i>	<i>P</i> 2 ₁ / <i>c</i>	<i>P</i> -1	<i>P</i> -1
<i>a</i> / Å	12.8955(3)	25.6756(7)	12.5928(4)	12.3371(4)	17.3190(5)	16.9431(4)
<i>b</i> / Å	19.5738(5)	19.1467(5)	18.4070(6)	11.2929(4)	19.9637(7)	20.0249(4)
<i>c</i> / Å	13.0841(3)	16.3667(4)	15.0348(5)	24.6580(7)	21.9686(8)	23.9395(5)
α / °	90	90	90	90	100.2942(18)	101.674(2)
β / °	101.9830(11)	107.328(2)	91.3592(14)	102.265(2)	91.2541(16)	105.876(2)
γ / °	90	90	90	90	115.3822(15)	118.124(5)
Volume / Å ³	3230.64(13)	7680.8(4)	3484.0(2)	3356.98(19)	6710.4(4)	6342.9(4)
<i>Z</i>	4	8	4	4	8	8
ρ_{calc} / g cm ⁻³	1.254	1.259	1.266	1.276	1.284	1.231
μ / mm ⁻¹	0.589	0.638	1.259	0.640	1.946	0.604
<i>F</i> (000)	1288	3088	1392	1364	2710	2480
Crystal size / mm ³	0.24×0.12×0.06	0.30×0.08×0.02	0.24×0.24×0.10	0.28×0.14×0.05	0.50×0.12×0.04	0.28×0.10×0.02
Radiation	CuK α	CuK α	CuK α	CuK α	CuK α	CuK α
θ range / °	4.13–67.15	2.93–66.86	3.80–66.82	3.67–64.65	2.51–67.41	2.70–67.68
Reflections collected	35356	56061	49855	39428	87157	83913
Independent refl.	5751	6821	6164	5930	23781	22486
<i>R</i> _{int}	0.0354	0.0907	0.0338	0.0548	0.0684	0.1577
G-of-F on <i>F</i> ²	1.03	1.03	1.05	1.04	1.03	1.02
Data/restraints/parameters	5751/0/426	6821/48/595	6164/0/469	5930/0/447	23781/18/1703	22486/0/1581
<i>R</i> 1 [<i>I</i> >2 σ (<i>I</i>)]	0.0400	0.0466	0.0424	0.0479	0.0725	0.0864
w <i>R</i> 2 [all data]	0.1023	0.1217	0.1094	0.1227	0.2039	0.2420
Largest diff. peak/hole / eÅ ⁻³	0.59/–0.35	0.24/–0.26	0.19/–0.52	0.27/–0.39	2.00/–0.92	1.02/–0.49

Crystallographic data: structures with *SQUEEZE* applied

In the moiety formula, parts enclosed in square brackets are assumed solvent content, consistent with the *SQUEEZE* results.

The empirical formula, formula weight, $F(000)$ and μ are modified to be consistent with the assumed moiety formula.

	4-Methylanisole (1:1)	Ethyl acetate	Et₂O/CHCl₃	Et₂O/MeCN	Et₂O/octanol	Et₂O/CH₂Cl₂
CCDC number	1827188	1827185	1827193	1827183	1827186	1827191
Empirical formula	C ₄₉ H ₃₉ NO ₂	C _{46.6} H _{40.2} NO _{3.8}	C _{47.4} H ₄₅ NO _{2.6}	C ₄₃ H ₃₄ NO _{1.5}	C ₄₇ H ₄₄ NO _{2.5}	C _{46.6} H ₄₃ NO _{2.4}
Moiety formula	C ₄₁ H ₂₉ NO, [C ₈ H ₁₀ O]	C ₄₁ H ₂₉ NO, [1.4(C ₄ H ₈ O ₂)]	C ₄₁ H ₂₉ NO, [1.6(C ₄ H ₁₀ O)]	C ₄₁ H ₂₉ NO, [0.5(C ₄ H ₁₀ O)]	C ₄₁ H ₂₉ NO, [1.5(C ₄ H ₁₀ O)]	C ₄₁ H ₂₉ NO, [1.4(C ₄ H ₁₀ O)]
<i>SQUEEZE</i> total electrons per unit cell	95	1201	1198	364	1134	1029
Formula weight	673.84	675.02	670.27	588.74	662.86	655.45
Temperature / K	180(2)	180(2)	180(2)	180(2)	180(2)	180(2)
Crystal system	monoclinic	trigonal	trigonal	trigonal	trigonal	trigonal
Space group	<i>P</i> 2 ₁ / <i>n</i>	<i>R</i> -3 <i>c</i>	<i>R</i> -3 <i>c</i>	<i>R</i> -3 <i>c</i>	<i>R</i> -3 <i>c</i>	<i>R</i> -3 <i>c</i>
<i>a</i> / Å	12.3591(3)	29.2539(11)	29.1890(6)	29.1831(6)	29.3589(6)	29.2009(5)
<i>b</i> / Å	18.2217(5)	29.2539(11)	29.1890(6)	29.1831(6)	29.3589(6)	29.2009(5)
<i>c</i> / Å	15.0443(4)	23.3293(9)	23.3065(5)	23.3144(5)	23.3712(5)	23.3366(4)
α / °	90	90	90	90	90	90
β / °	91.6057(11)	90	90	90	90	90
γ / °	90	120	120	120	120	120
Volume / Å ³	3386.70(15)	17290.2(15)	17196.7(8)	17195.6(8)	17445.8(8)	17233.0(7)
<i>Z</i>	4	18	18	18	18	18
ρ_{calc} / g cm ⁻³	1.322	1.167	1.165	1.023	1.136	1.137
μ / mm ⁻¹	0.62	0.58	0.55	0.47	0.54	0.53
<i>F</i> (000)	1424	6429.6	6429.6	5598	6354	6278.4
Crystal size / mm ³	0.30×0.28×0.10	0.30×0.16×0.12	0.18×0.16×0.04	0.25×0.14×0.12	0.26×0.20×0.08	0.30×0.18×0.10
Radiation	CuK α	CuK α	CuK α	CuK α	CuK α	CuK α
θ range / °	3.81–66.86	3.02–66.95	3.02–66.72	3.03–66.79	3.01–66.73	3.03–66.81
Reflections collected	49031	63518	60892	52403	49809	45494
Independent refl.	5990	3428	3397	3402	3445	3410
<i>R</i> _{int}	0.0298	0.0587	0.1267	0.0432	0.0501	0.0680
G-of-F on <i>F</i> ²	1.08	1.04	1.03	1.05	1.06	1.04
Data/restraints/parameters	5990/0/389	3428/0/198	3397/0/198	3402/0/198	3445/0/198	3410/0/198
<i>R</i> 1 [<i>I</i> >2 σ (<i>I</i>)]	0.0387	0.0397	0.0536	0.0487	0.0410	0.0398
w <i>R</i> 2 [all data]	0.1139	0.1164	0.1569	0.1465	0.1116	0.1154
Largest diff. peak/hole / eÅ ⁻³	0.19/–0.19	0.22/–0.18	0.19/–0.19	0.24/–0.25	0.22/–0.17	0.16/–0.14

Summary of structure types for Reichardt's dye

	CCDC	Space group	a (Å)	b (Å)	c (Å)	a (°)	b (°)	g (°)	V (Å ³)
Hexagonal pore structure	1827185	R-3c	29.2539(11)	29.2539(11)	23.3293(9)	90	90	120	17290.2(15)
	1827193		29.1890(6)	29.1890(6)	23.3065(5)	90	90	120	17196.7(8)
	1827183		29.1831(6)	29.1831(6)	23.3144(5)	90	90	120	17195.6(8)
	1827186		29.3589(6)	29.3589(6)	23.3712(5)	90	90	120	17445.8(8)
	1827191		29.2009(5)	29.2009(5)	23.3366(4)	90	90	120	17233.0(7)
Acetone solvate (1:1)	1827182	P21/n	12.8955(3)	19.5738(5)	13.0841(3)	90	101.983(1)	90	3230.64(13)
Dioxane solvate (1:2)	1827192	C2/c	25.6756(7)	19.1467(5)	16.3667(4)	90	107.328(2)	90	7680.8(4)
Chlorobenzene (1:1)	1827190	P21/n	12.5928(4)	18.4070(6)	15.0348(5)	90	91.359(1)	90	3484.0(2)
4-Methylanisole (1:1)	1827188	P21/n	12.3591(3)	18.2217(5)	15.0443(4)	90	91.6057(11)	90	3386.70(15)
Ethylene glycol solvate (2:3)	1827184	P21/c	12.3371(4)	11.2929(4)	24.6580(7)	90	102.265(2)	90	3356.98(19)
CHCl ₃ /H ₂ O solvate (1:0.625:1.25)	1827187	P-1	17.3190(5)	19.9637(7)	21.9686(8)	100.2942(18)	91.2541(16)	115.3822(15)	6710.4(4)
H ₂ O(MeOH) solvate ^a	1827189	P-1	16.9431(4)	20.0249(4)	23.9395(5)	101.674(2)	105.876(2)	118.124(5)	6342.9(4)
Ethanol (1:1) ^b	PUTMOH	P21/n	10.1428(3)	19.0295(6)	17.0312(5)	90	102.607(2)	90	3207.98(17)
i-Propanol (1:1) ^b	PUTMAN	P21/n	10.4500(7)	19.7456(11)	16.6334(9)	90	105.934(3)	90	3300.3(3)

^a Crystal grown from MeOH. Solvent content appears from X-ray diffraction to be H₂O.

^b **Isostructural**. Published previously: S.Kurjatschij, W.Seichter, E.Weber, *New J.Chem.* (2010), **34**, 1465.

Table S1. Summary of structure types for Reichardt's dye.

2. Intermolecular interactions in the hexagonal channel structure

Figure S1. The hexagonal channel structure is built from one key intermolecular interaction, which places one phenyl ring above the pyridinium ring of an adjacent molecule, with the C–O⁻ group accepting C–H···O hydrogen bonds¹ from three phenyl rings. Perpendicular views of the interaction are as follows:

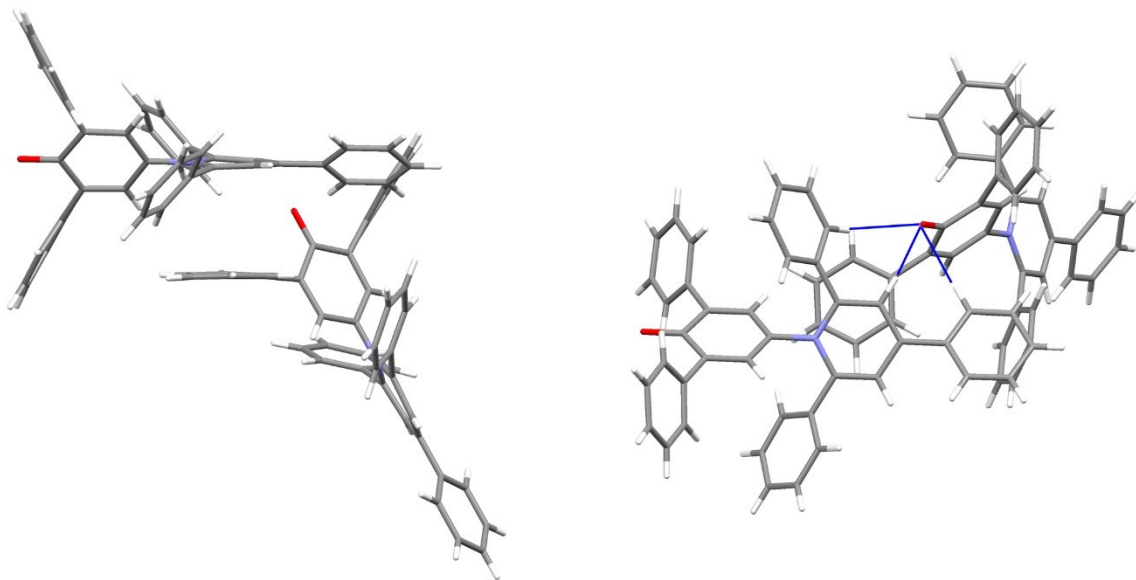


Figure S2. A 120° angle is adopted between the central cores of the interacting dye molecules, which are arranged into rings in the hexagonal channel structure:

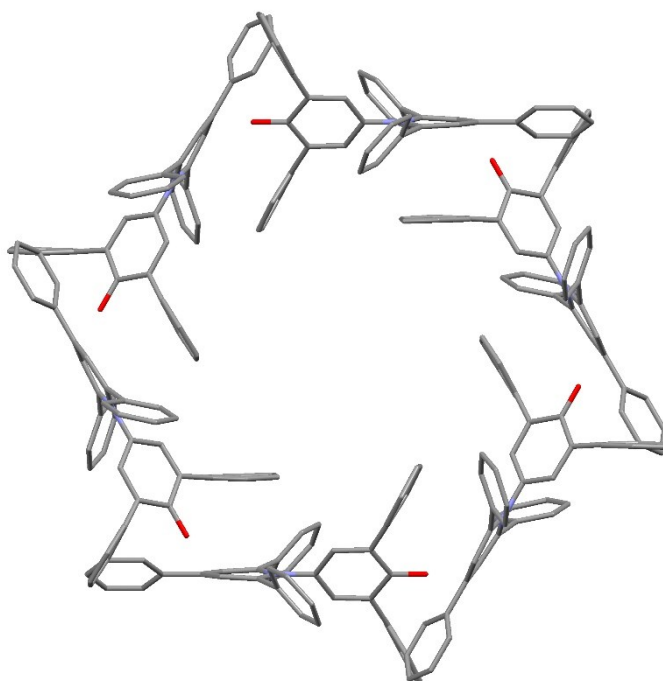
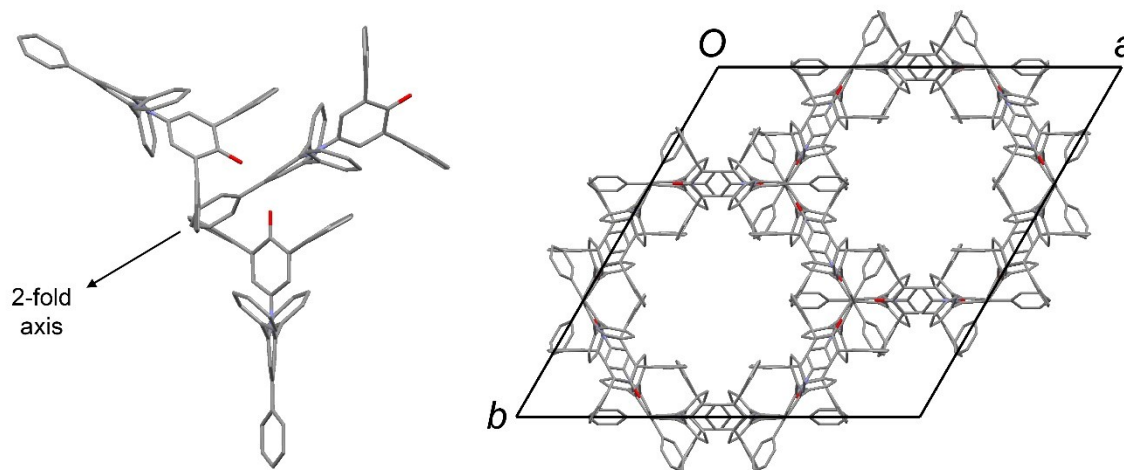


Figure S3. Each dye molecule is involved in **two** interactions around its central pyridinium ring, related by a 2-fold rotation about the long axis of the central core of the molecule (*i.e.* along the C–O⁻ bond), producing a “trigonal node” that enables formation of the observed 3-D channel structure:



3. Intermolecular interactions in the chlorobenzene/4-methylanisole structures

Figure S4. The chlorobenzene and 4-methylanisole structures are isostructural. The structure (coloured red in the diagram below) contains the same intermolecular interactions as in the hexagonal structure, defining 1-D sections along the *ac* diagonal of the unit cell, which are **identical** to those in the hexagonal structure (coloured blue below):

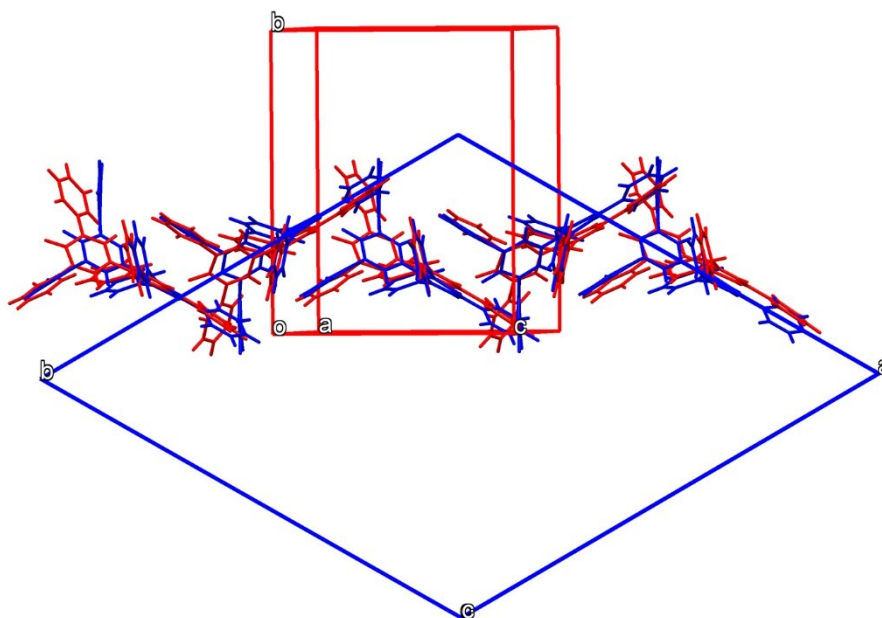


Figure S5. In the chlorobenzene/4-methylanisole structures, the other side of each pyridinium ring is capped by a solvent molecule, which precludes formation of the trigonal node that exists in the hexagonal channel structure. The chlorobenzene/4-methylanisole structure comprises layers of Reichardt's dye molecules in the *ac* planes of the unit cell, which are **polar** (i.e. all C–O⁻ groups are oriented in the same direction along the *c* axis):

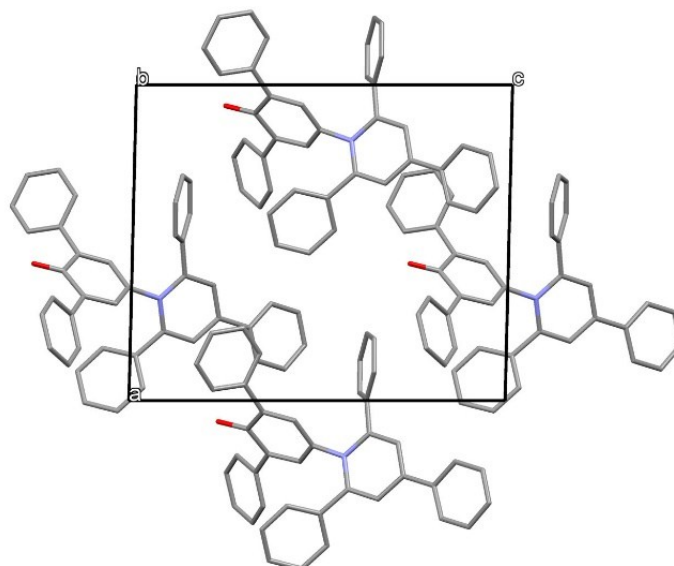
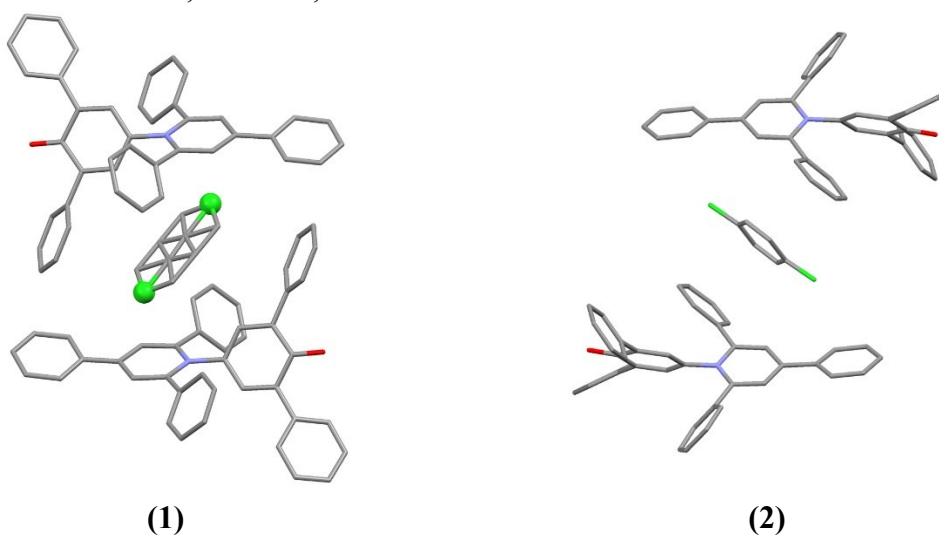


Figure S6. These polar layers are stacked with inversion centres between them, with the chlorobenzene or 4-methylanisole molecules between the layers, as indicated in Fig. 3 of the main paper. In the 4-methylanisole crystal structure, the electron density appears as disordered rods along the *a*-axis. It is difficult to model discrete 4-methylanisole molecules, so the structure was finally treated with *SQUEEZE*.² For the chlorobenzene structure, however, two clear molecular sites are identified:



- (1) A disordered centrosymmetric site between two pyridinium rings, with the Cl atom of chlorobenzene (highlighted) pointing towards N⁺ in either of the two neighbouring rings.
- (2) A disordered centrosymmetric site sandwiched between two phenyl rings.

4. Polar aprotic O-containing solvents: acetone and dioxane

Figure S7. The crystal structures containing acetone and dioxane include intermolecular interactions similar to those seen in the hexagonal channel structure, but with one molecule **reflected** (red = acetone structure, blue = hexagonal structure):

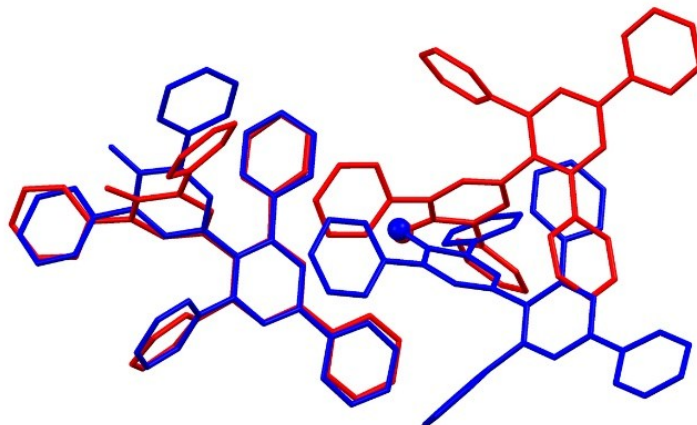


Figure S8. The position of the O atom accepting the C–H···O H-bonds is consistent in each case (highlighted by the ball in the diagram above), but one of the phenyl rings donating a C–H···O H-bond to O within the hexagonal structure is turned so that it donates its H atom instead to a neighbouring phenyl ring:

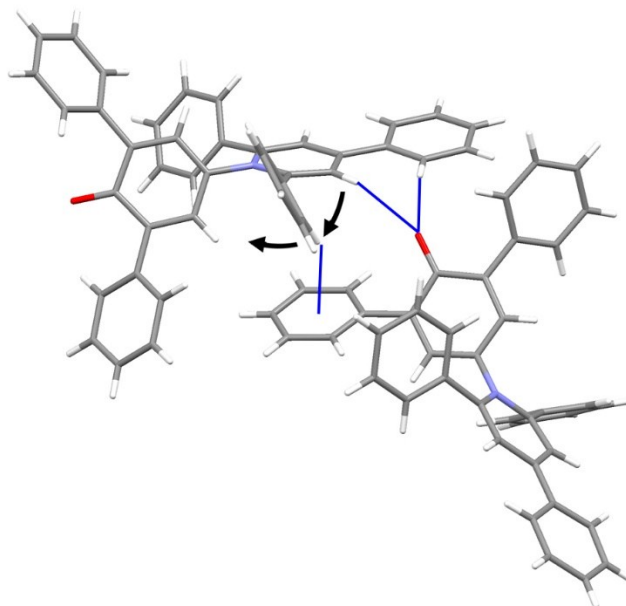
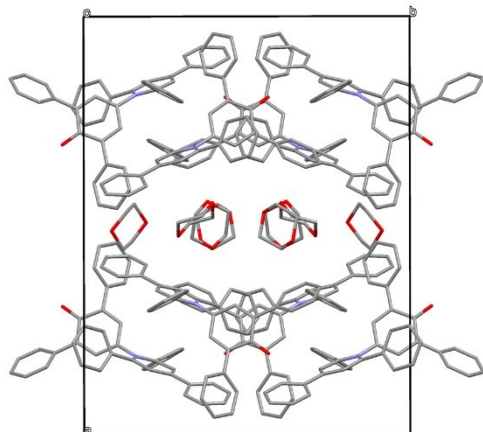
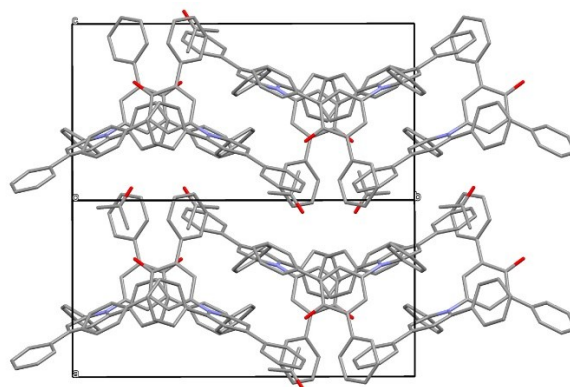


Figure S9. The acetone and dioxane structures contain **identical 2-D sections** based on this motif, defined in the (10–1) planes in the acetone structure and in the bc planes in the dioxane structure (horizontal in the diagrams below). These 2-D sections are stacked differently in the two cases, forming clear channels in the dioxane structure, but a more condensed structure for acetone:

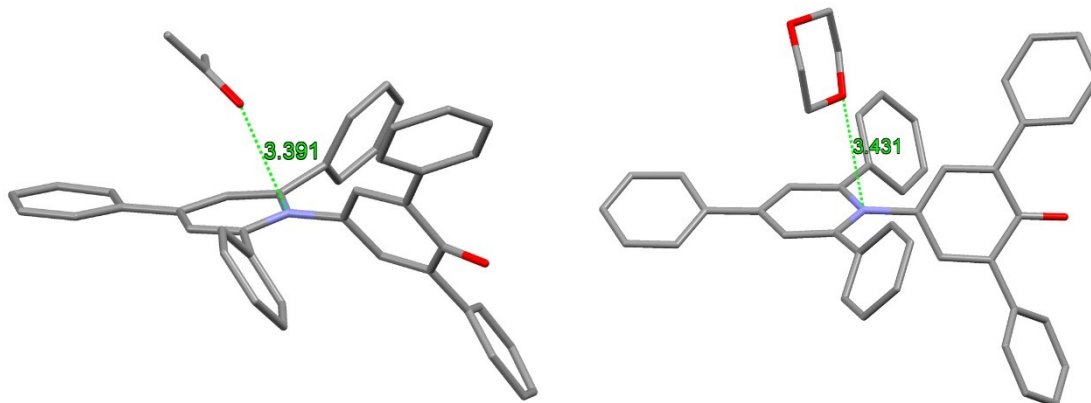


Dioxane
2-D sections in the bc planes
(horizontal)
Sections are stacked to define
channels



Acetone
2-D sections in (10–1) (horizontal)
Sections are stacked with “Bumps meeting
hollows”

Figure 10. In both cases, the solvent molecules interact with the pyridinium ring of Reichardt’s dye by directing their O atom towards N⁺. The geometry of each contact clearly corresponds to the direction expected for the lone pair of electrons on O.



The dioxane molecules show extensive disorder in space group C2/c, but their positions can be quite clearly unravelled. An expanded version of the structure is included in the accompanying CIF, showing the full unit-cell contents with one ordered representation of the local arrangement of dioxane molecules. The dioxane molecules do not directly “pillar” the structure by one molecule linking between two pyridinium rings in adjacent 2-D sections, but the different bulk of dioxane compared to acetone must clearly contribute to the observed differences between the structures.

5. Protic solvents: ethylene glycol, EtOH, ⁱPrOH, H₂O(MeOH), CHCl₃/H₂O

In the three new structures containing protic solvents, and in the previously-reported EtOH and ⁱPrOH structures, the O atom of Reichardt's dye accepts at least one H-bond from the solvent.

Figure S11. The EtOH and ⁱPrOH structures (which are isostructural), contain Reichardt's dye molecules lying in 2-D sections in the (10-1) planes that are **identical to those described for acetone and dioxane**, and the structures of the EtOH/ⁱPrOH (shown in blue below) and acetone (shown in red below) solvates appear essentially identical in projection:

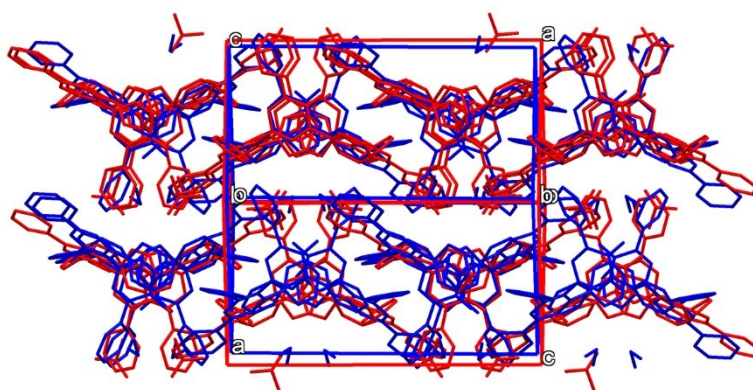
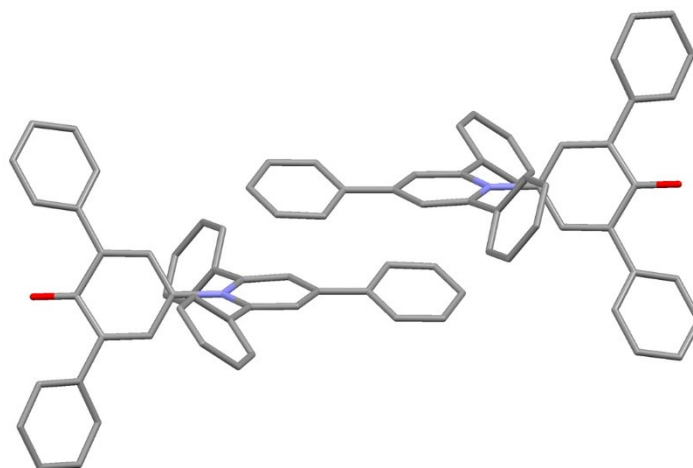


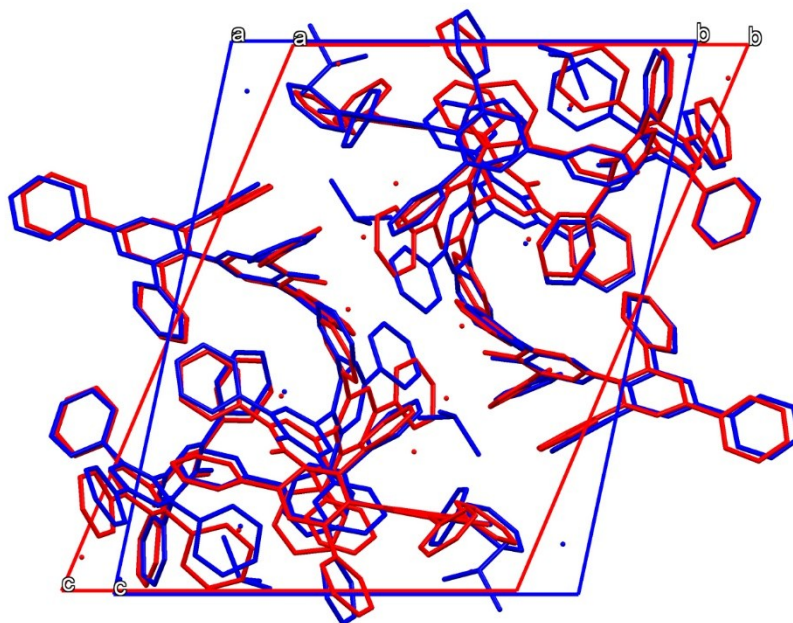
Figure S12. The 2-D sections are stacked differently, however, and the alcohol molecules lie in pockets between pendant phenyl rings; they do not have any close contacts to the pyridinium ring of Reichardt's dye. The dye molecules are instead involved in centrosymmetric contacts:



Polytypism in the $\text{CHCl}_3/\text{H}_2\text{O}$ and $\text{H}_2\text{O}(\text{MeOH})$ solvates

This $\text{H}_2\text{O}(\text{MeOH})$ structure is a polytype of the $\text{CHCl}_3/\text{H}_2\text{O}$ structure. The unit cell of the $\text{H}_2\text{O}(\text{MeOH})$ structure has been chosen to emphasise this polytypic relationship (it is not the reduced cell). Sections in the ab planes are identical in the two structures, but the c axis is defined differently (corresponding to an offset of adjacent sections roughly perpendicular to the b axis).

Figure S13. An overlay of the unit-cell contents for the two structures ($\text{H}_2\text{O}(\text{MeOH})$ red, $\text{CHCl}_3/\text{H}_2\text{O}$ blue) is as follows:



Intermolecular interactions for single crystals grown from the vapour diffusion of hexane into a solution of Reichardt's dye in ethylene glycol

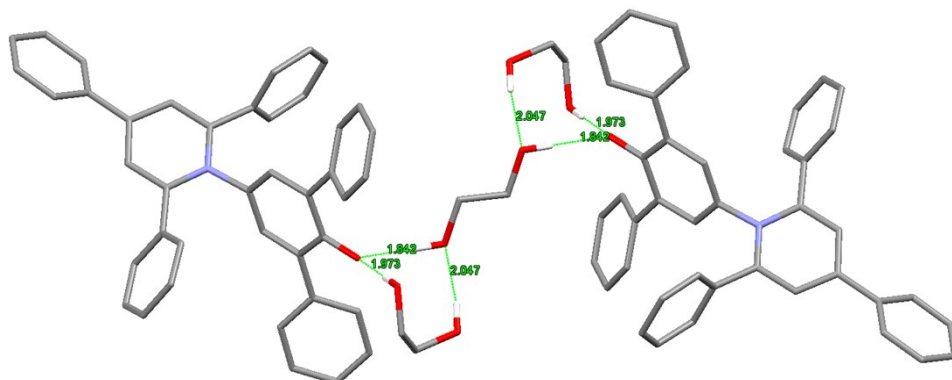


Figure S14. Two intermolecular HO--O H-bonding interactions are observed between two different solvent molecules (ethylene glycol) and Reichardt's dye (1.973 Å and 1.943 Å) and one intermolecular HO--O interaction is observed between two solvent molecules (2.047 Å). N atoms are shown in light blue, O atoms are shown in red, C atoms are shown in grey and H atoms are shown in white. Only H atoms on the ethylene glycol solvent molecules which participate in H-bonding interactions with Reichardt's dye or another solvent molecule are shown for clarity.

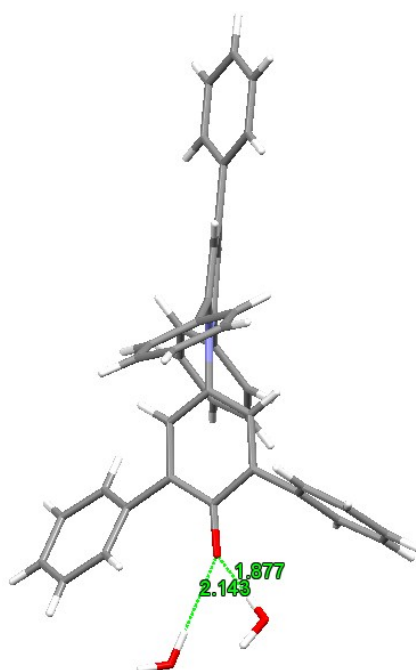


Figure S15. Bifurcated “three-centre” intermolecular HO--O H-bonding interaction³ observed between the phenolate oxygen of Reichardt's dye and the hydroxyl group of two different water molecules. (2.143 Å and 1.877 Å). N atoms are shown in light blue, O atoms are shown in red, C atoms are shown in grey and H atoms are shown in white.

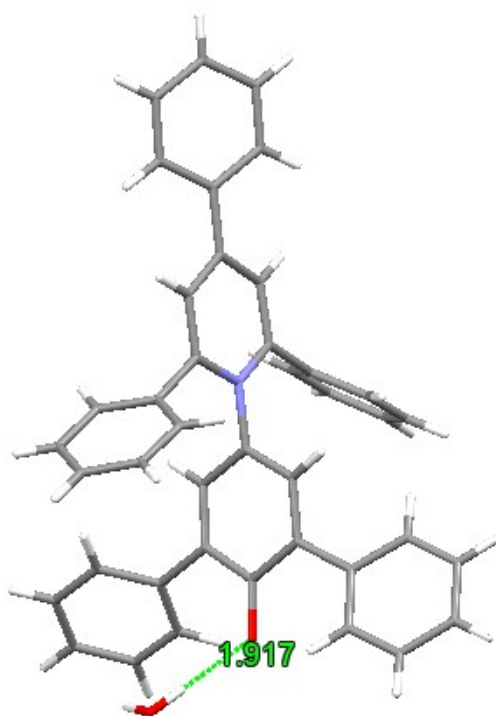


Figure S16. One intermolecular HO--O H-bonding interaction observed between the phenolate oxygen of Reichardt's dye and the hydroxyl group of a water molecule. (1.917 Å). N atoms are shown in light blue, O atoms are shown in red, C atoms are shown in grey and H atoms are shown in white.

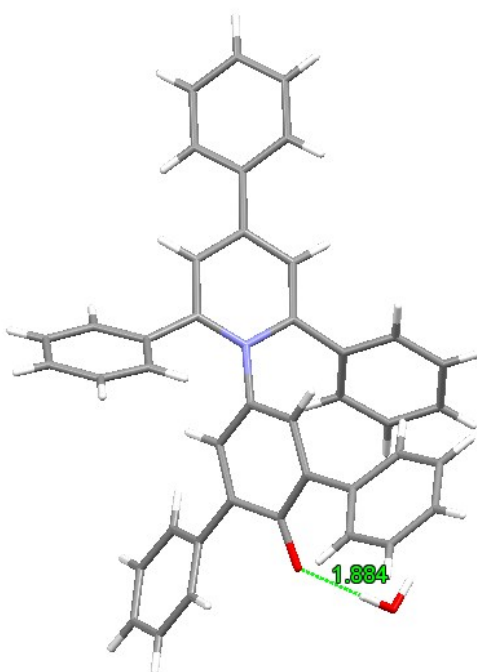


Figure S17. One intermolecular HO--O H-bonding interaction observed between the phenolate oxygen of Reichardt's dye and the hydroxyl group of a water molecule. (1.884 Å). N atoms are shown in light blue, O atoms are shown in red, C atoms are shown in grey and H atoms are shown in white.

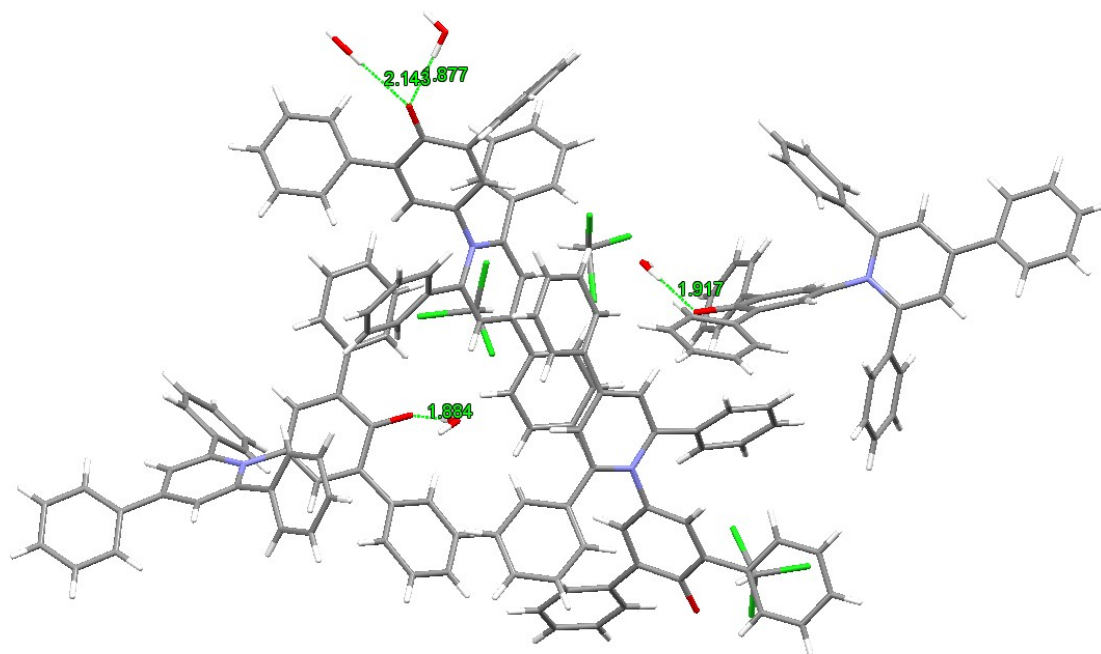


Figure S18. Packing of the water molecules and Reichardt's dye involved in intermolecular H-bonding interactions. Four intermolecular HO--O H-bonding interactions are observed between the phenolate oxygen of Reichardt's dye and the hydroxyl group of water molecules. One intermolecular HO--O H-bonding interaction is observed between one water molecule and Reichardt's dye (1.884 Å), another HO--O H-bonding interaction is observed between different water molecule and a different molecule of Reichardt's dye (1.917 Å) and finally two intermolecular HO--O H-bonding interactions are observed to the phenolate oxygen of a different molecule of Reichardt's dye and two different water molecules (2.143 Å and 1.877 Å). Cl atoms are shown in bright green, N atoms are shown in light blue, O atoms are shown in red, C atoms are shown in grey and H atoms are shown in white.

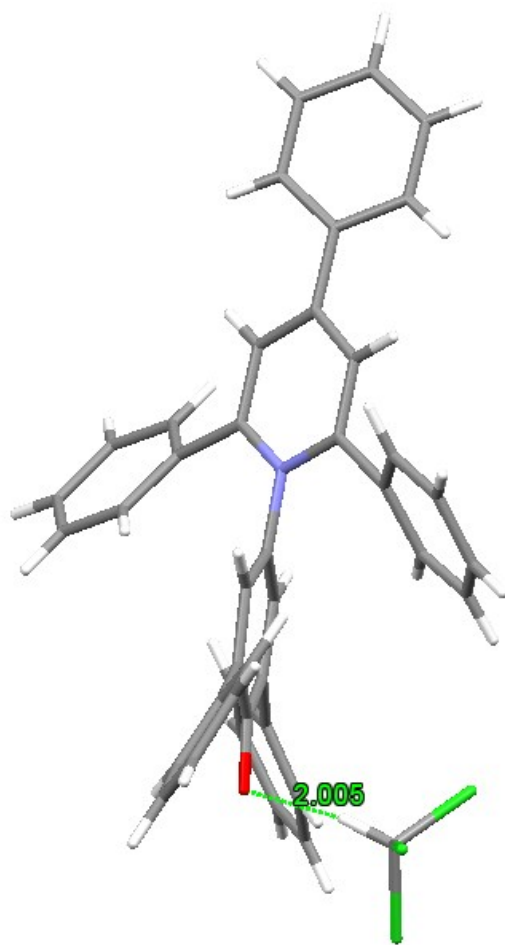


Figure S19. One intermolecular Cl₃CH...O H-bonding interaction observed between the phenolate oxygen of Reichardt's dye and the H atom of a chloroform solvent molecule (2.005 Å).⁴ Cl atoms are shown in light green, N atoms are shown in light blue, O atoms are shown in red, C atoms are shown in grey and H atoms are shown in white.

Presence of water cluster for single crystals grown from the vapour diffusion of hexane into a solution of Reichardt's dye in ethylene glycol

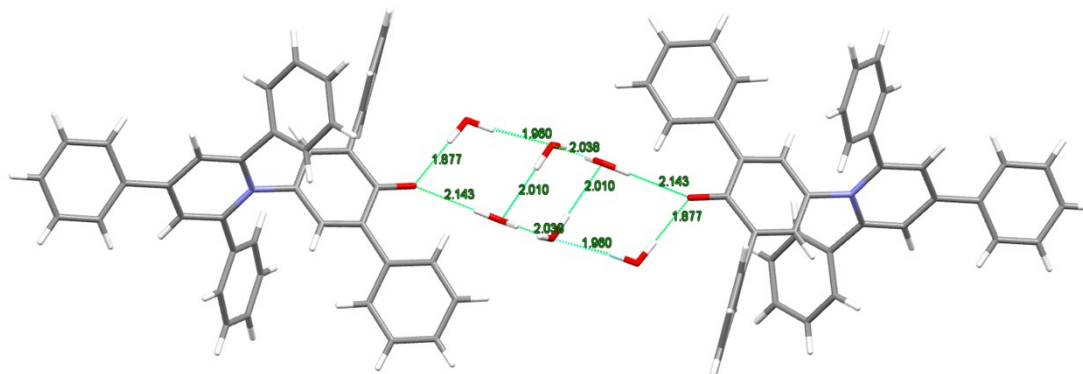


Figure S20. H-bonded water cluster⁵ involving six water molecules and two molecules of Reichardt's dye. Four intermolecular HO--O H-bonding interactions are observed between two different solvent molecules (water) and Reichardt's dye (2.143 Å and 1.877 Å) and six intermolecular HO--O H-bonding interactions are observed between six water molecules (2.010 Å, 1.960 Å and 2.039 Å). There is a plane of symmetry down the centre of the water cluster. N atoms are shown in light blue, O atoms are shown in red, C atoms are shown in grey and H atoms are shown in white.

6. Tunnel Calculations Using CAVER 3.0

The crystal structures were prepared for tunnel calculations by removing the solvent molecules. Tunnels were calculated in each structure using CAVER3.0.⁶ Structural analysis and figure preparations were done with PyMOL.⁷

Tunnel Calculation Using CAVER3.0 for Single Crystals Grown of Reichardt's Dye from Chloroform/Et₂O

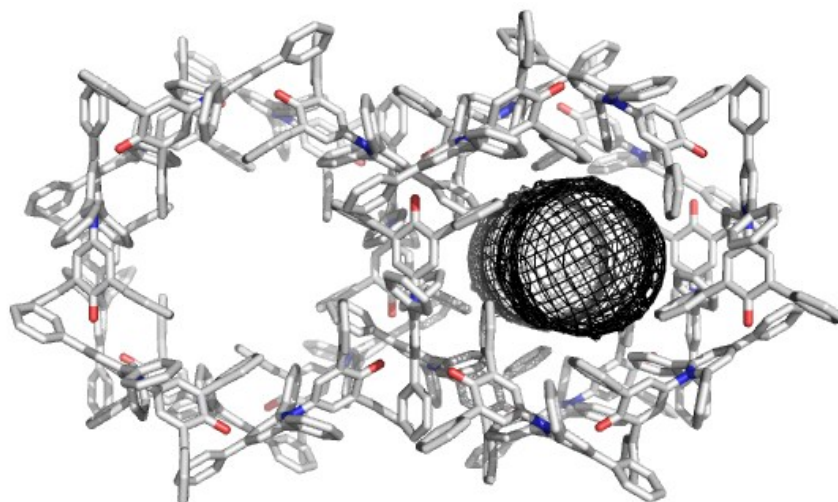


Figure S21. Packing arrangement in single crystals of **1** obtained by vapour diffusion of diethyl ether into a solution of **1** in chloroform displaying the 7.2 Å hexagonal channel structure as viewed along the *c* axis. The channels contain disordered solvent, and the dimensions of the channel are illustrated using the mesh image calculated using CAVER3.0 (right).⁶ O atoms are shown in red, N atoms in light blue and C atoms in grey. H atoms are omitted for clarity. The bottleneck radius of the channel is calculated to be 3.6 Å using CAVER3.0.⁸

Tunnel Calculations Using CAVER3.0 for Single Crystals Grown of Reichardt's Dye from Vapour Diffusion of Hexane into a Solution of Reichardt's Dye in 1,4-dioxane

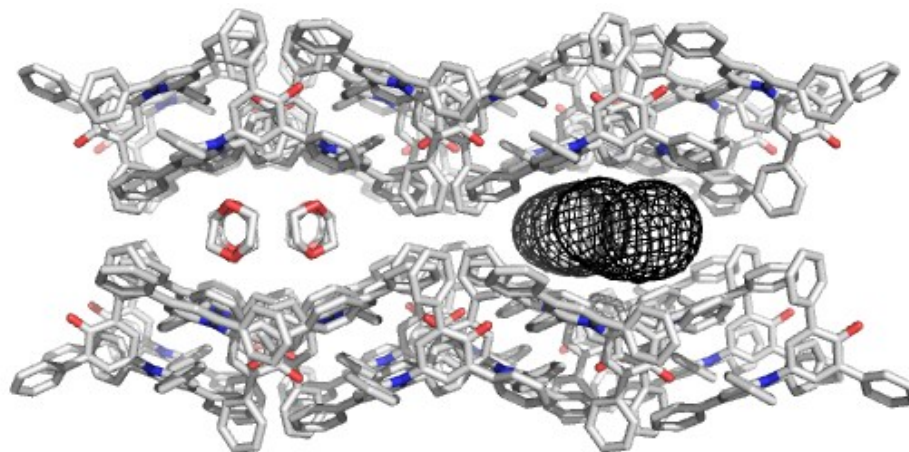


Figure S22. Packing arrangement in single crystals of **1** obtained by vapour diffusion of hexane into a solution of **1** in 1,4-dioxane displaying the 4.6 Å channel structure as viewed along the *c* axis. The channels are filled with disordered solvent molecules, and the dimensions of the channel are illustrated using the mesh image calculated using CAVER3.0 (right).⁶

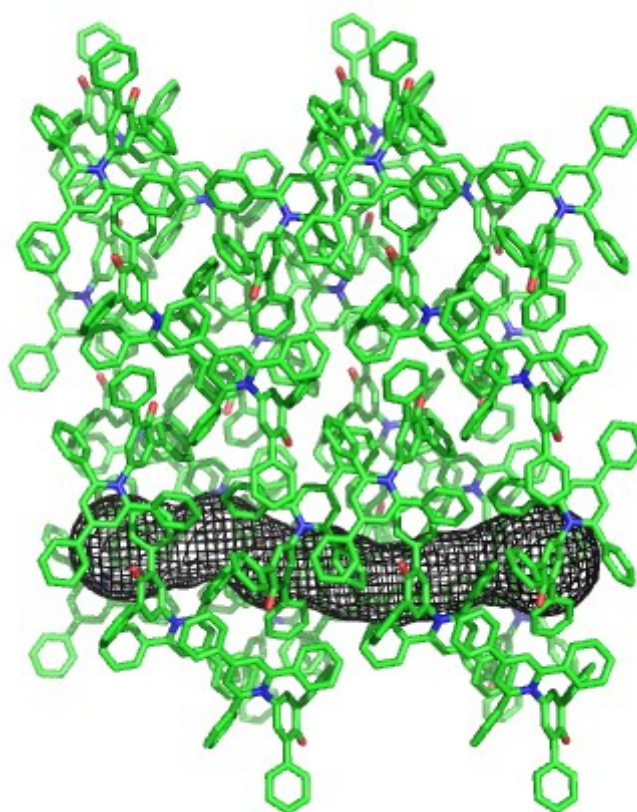


Figure S23. Packing arrangement in single crystals of **1** obtained by vapour diffusion of hexane into a solution of **1** in 1,4-dioxane displaying the channel structure as viewed side-on. The pore at the top shows the empty cavity and at the bottom displays the channel as determined by CAVER3.0 once the disordered solvents molecules had been removed.⁶ O atoms are shown in red, N atoms in light blue and C atoms in green. H atoms have been omitted for clarity. The dimensions of the channel are illustrated using the mesh image calculated using CAVER3.0 (right).

**Tunnel Calculation Using CAVER3.0 for Single Crystals Grown of Reichardt's
Dye from the Slow Evaporation of Ethyl Acetate**

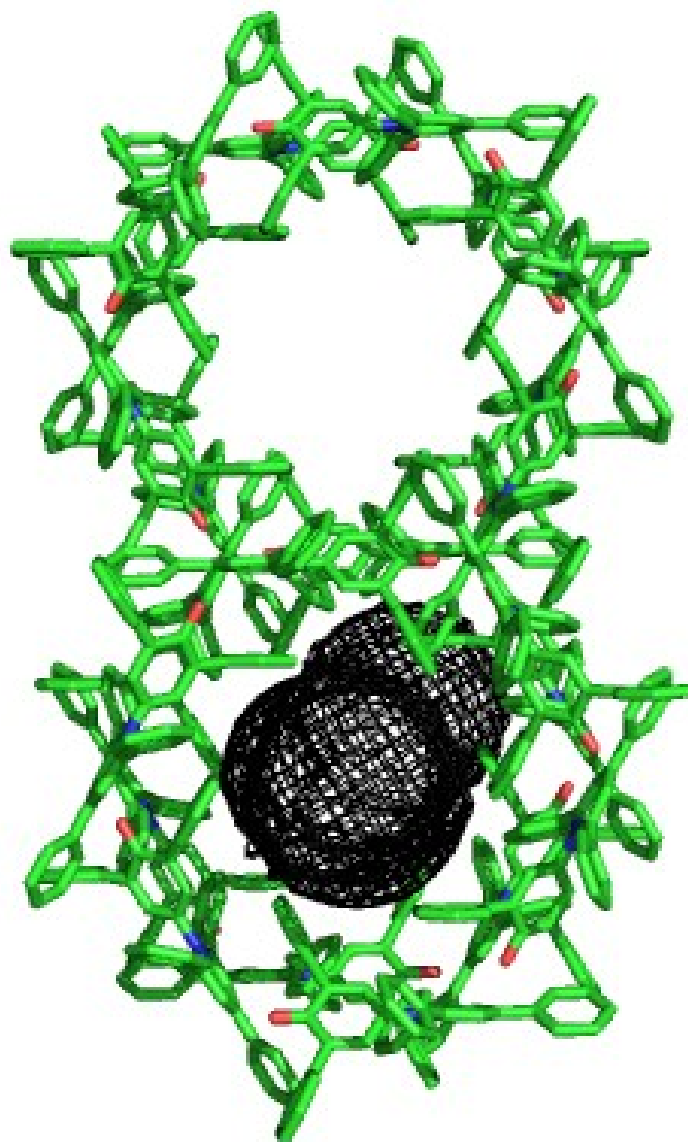


Figure S24. Packing arrangement in single crystals of **1** obtained by the slow evaporation of ethyl acetate from a solution of **1** displaying the hexagonal channel structure as viewed along the *c* axis. The top pore shows an empty cavity and the bottom pore displays the channel as determined by CAVER3.0.⁶ O atoms are shown in red, N atoms in light blue and C atoms in green. H atoms are omitted for clarity. The calculated channel is shown as a black mesh. The bottleneck radius of the channel is calculated to be 3.6 Å using CAVER3.0.

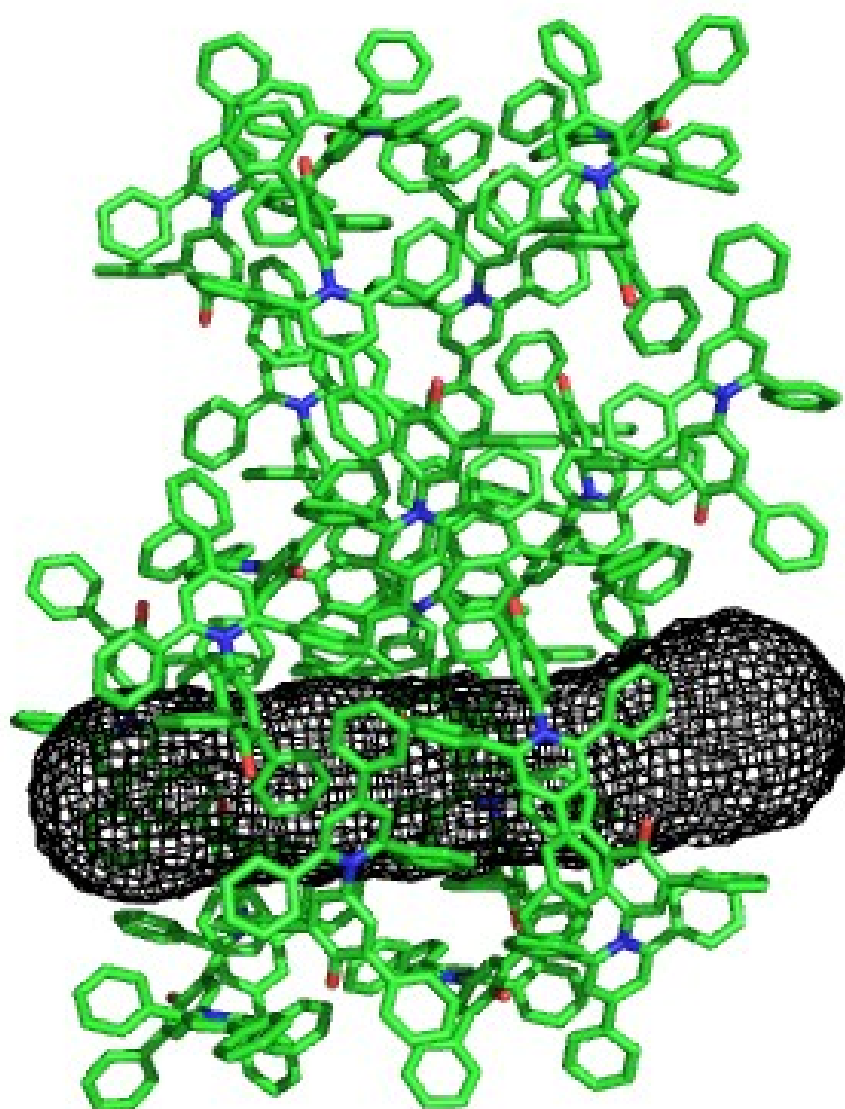


Figure S25. Packing arrangement in single crystals of **1** obtained by the slow evaporation of ethyl acetate from a solution of **1** displaying the hexagonal channel structure as viewed side-on. The top pore shows an empty cavity and the bottom pore displays the channel as determined by CAVER3.0.⁶ O atoms are shown in red, N atoms in light blue and C atoms in green. H atoms are omitted for clarity. The calculated channel is shown as a black mesh. The bottleneck radius of the channel is calculated to be 3.6 Å using CAVER3.0.⁸

Tunnel Calculations Using CAVER3.0 for Single Crystals Grown of Reichardt's Dye from the Vapour Diffusion of Di-ethyl ether into a Solution of 1 in Acetonitrile

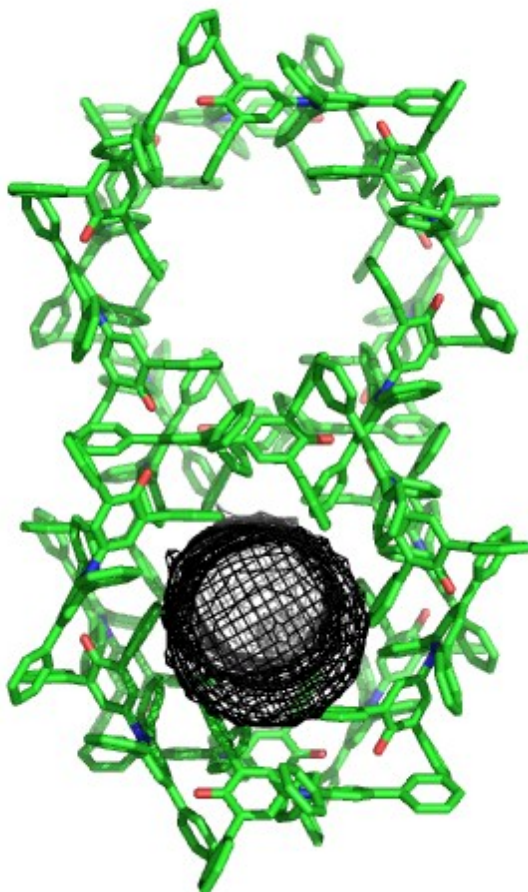


Figure S26. Packing arrangement in single crystals of **1** obtained from a solution of **1** in acetonitrile with the vapour diffusion of di-ethyl ether displaying the hexagonal channel structure as viewed along the *c* axis. The top pore shows an empty cavity and the bottom pore displays the channel as determined by CAVER3.0.⁶ O atoms are shown in red, N atoms in light blue and C atoms in green. H atoms are omitted for clarity. The calculated channel is shown as a black mesh. The bottleneck radius of the channel is calculated to be 3.43 Å using CAVER3.0.⁸

Tunnel Calculations Using CAVER3.0 for Single Crystals Grown of Reichardt's Dye from the Vapour Diffusion of Di-ethyl ether into a Solution of **1 in Dichloromethane**

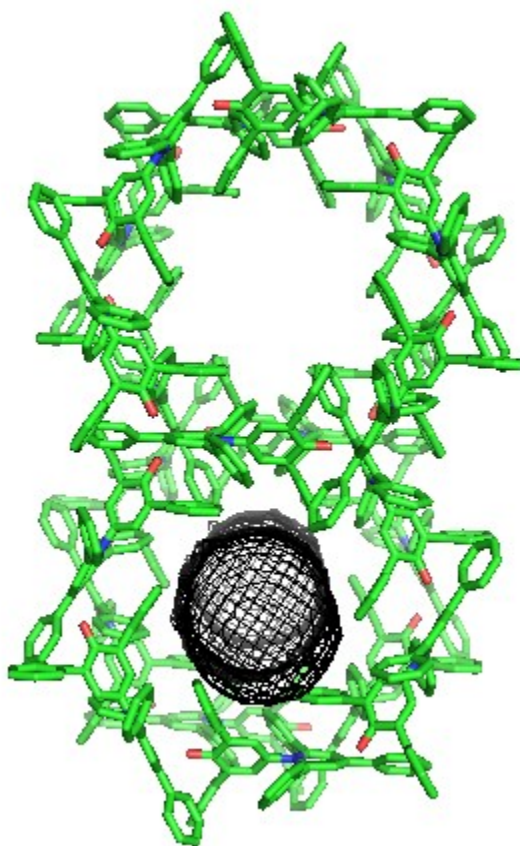


Figure S27. Packing arrangement in single crystals of **1** obtained by vapour diffusion of diethyl ether into a solution of **1** in dichloromethane displaying the hexagonal channel structure as viewed along the *c* axis. The top pore shows an empty cavity and the bottom pore displays the channel as determined by CAVER3.0.⁶ O atoms are shown in red, N atoms in light blue and C atoms in green. H atoms are omitted for clarity. The calculated channel is shown as a black mesh. The bottleneck radius of the channel is calculated to be 3.62 Å using CAVER3.0.⁸

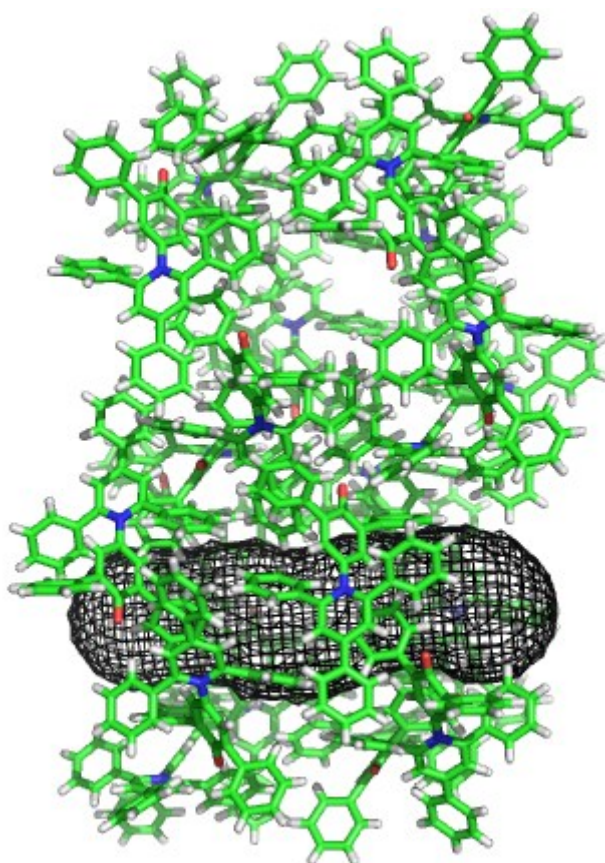


Figure S28. Packing arrangement in single crystals of **1** obtained by vapour diffusion of diethyl ether into a solution of **1** in dichloromethane displaying the hexagonal channel structure as viewed side-on. The top pore shows an empty cavity and the bottom pore displays the channel as determined by CAVER3.0.⁶ O atoms are shown in red, N atoms in light blue, C atoms in green and H atoms in white. The calculated channel is shown as a black mesh. The bottleneck radius of the channel is calculated to be 3.62 Å using CAVER3.0.⁸

Tunnel Calculations Using CAVER3.0 for Single Crystals Grown of Reichardt's Dye from the Slow Evaporation of Chlorobenzene

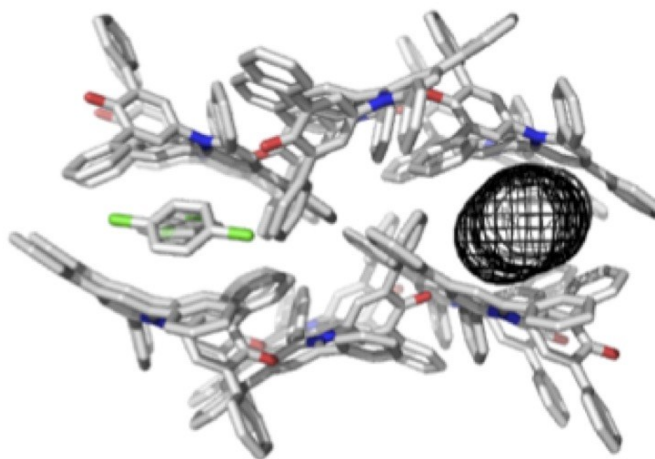


Figure S29. Packing arrangement in single crystals of **1** obtained by slow evaporation of chlorobenzene displaying the 4.0 Å channel structure as viewed along the *a* axis. The channels are filled with disordered solvent molecules, and the dimensions of the channel are illustrated using the mesh image calculated using CAVER3.0 (right).⁶

Tunnel Calculation Using CAVER3.0 for single crystals of Reichardt's Dye Grown from the Vapour Diffusion of Di-ethyl ether into a Solution of **1 in 1-octanol**

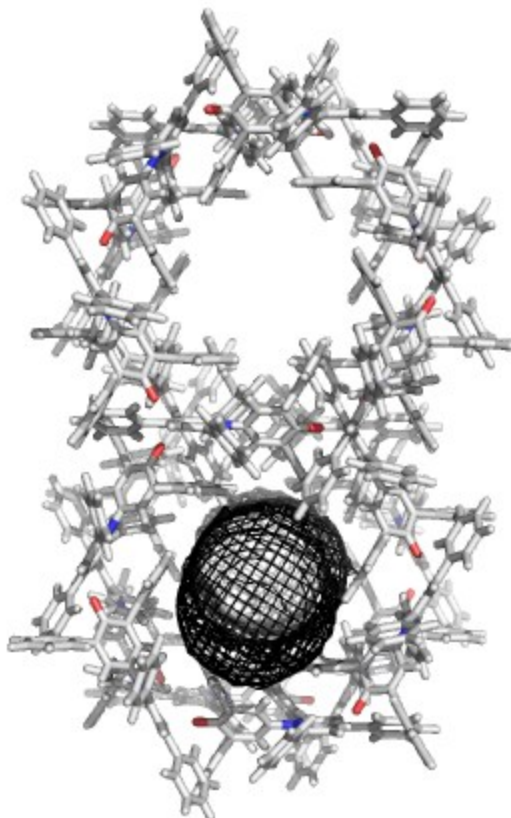


Figure S30. Packing arrangement in single crystals of **1** obtained by vapour diffusion of diethyl-ether into a solution of **1** in 1-octanol displaying the hexagonal channel structure as viewed along the *c* axis. The top pore shows an empty cavity and the bottom pore displays the channel as determined by CAVER3.0.⁶ O atoms are shown in red, N atoms in light blue and C and H atoms in grey. The calculated channel is shown as a black mesh. The bottleneck radius of the channel is calculated to be 3.59 Å using CAVER3.0.⁸

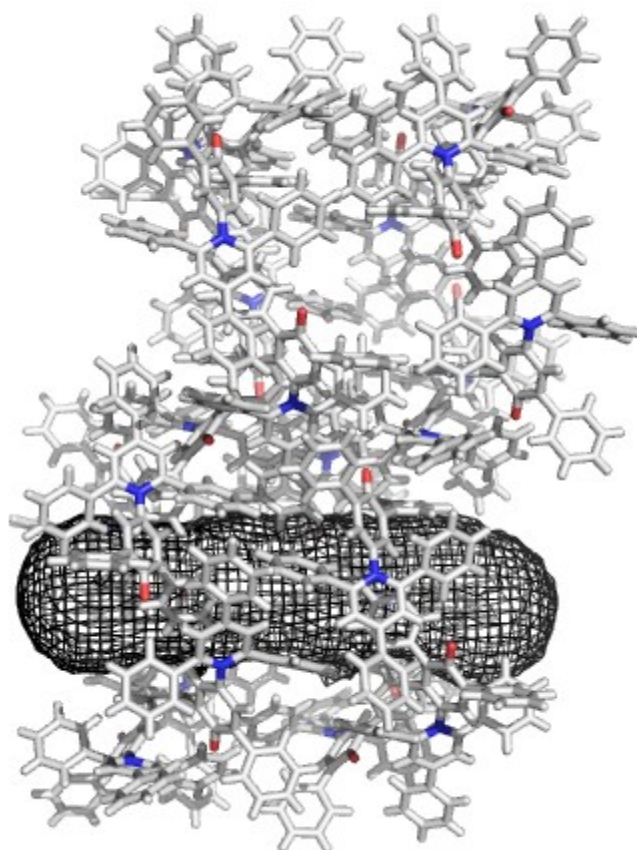


Figure S31. Packing arrangement in single crystals of **1** obtained by vapour diffusion of diethyl ether into a solution of **1** in 1-octanol displaying the hexagonal channel structure as viewed side-on. The top pore shows an empty cavity and the bottom pore displays the channel as determined by CAVER3.0.⁶ O atoms are shown in red, N atoms in light blue and C and H atoms in grey. The calculated channel is shown as a black mesh. The bottleneck radius of the channel is calculated to be 3.59 Å using CAVER3.0.⁸

8. References

- 1 S. Horowitz and R. C. Trievel, *J. Biol. Chem.*, 2012, **287**, 41576-41582.
- 2 PLATON SQUEEZE has been employed to calculate the disordered solvent contribution to the structure; see A. L. Spek, *Acta. Cryst.*, 2015, **C71**, 9.
- 3 I. Rozas, I. Alkorta and J. Elguero, *J. Phys. Chem. A.*, 1998, **102**, 9925.
- 4 N. Goutev and H. Matsuura, *J. Phys. Chem. A.*, 2001, **105**, 4741.
- 5 (a) G. K. Ghosh and P. K. Bharadwaj, *Inorg. Chem.*, 2012, **43**, 5180; (b) N. S. Oxtoby, A. J. Blake, N. R. Champness and C. Wilson, *Chem. Eur. J.*, 2005, **11**, 4643.
- 6 E. Chovancová, A. Pavelka, P. Beneš, O. Strnad, J. Brezovsky, B. Kozlikova, A. Gora, V. Sustr, M. Klvana, P. Medek, L. Biedermannova, J. Sochor, J. Damborsky, *PLoS Comput. Biol.*, 2012, **8**, 10.
- 7 The PyMOL Molecular Graphics System, Version 1.4.1, Schrödinger.
- 8 CAVER3.0 was used to determine the narrowest point along the channel, termed the bottleneck, and the internal diameter is quoted as twice the bottleneck radius.